AN EXPERIMENTAL STUDY OF THE COMPLEX DYNAMIC MODULUS

Flight Lieutenant Graeme G. Wren
(Royal Australian Air Force)
and
Dr Vikram K. Kinra
Aerospace Engineering Department
Texas A&M University
College Station, Texas, 77843
(409) 845-1667

ABSTRACT

An overview of an experimental program for determining the dynamic flexural constitution of materials is presented. This program entails the development of a fully-automated flexural apparatus, its calibration, and studies of structural damping and dynamic flexural modulus of a variety of materials. Furthermore, Graphite/Aluminum laminates, $[\pm\theta]_s$, with θ ranging from zero to ninety in fifteen degree increments, were tested. Classical laminate theory and the work of Ni and Adams was found to adequately predict both the modulus and the damping. It is demonstrated that the attachment of an end-mass (to vary the resonant frequency) does not contribute to the measured damping.

KEYWORDS: Damping, modulus, composite material, flexural, structural, dynamic, experimental, logarithmic decrement, vacuum.

SYMBOLS USED

A = cross sectional area of beam, amplitude
C_p = specific heat per unit mass at constant pressure
D_{ij} = components of the flexural modulus matrix for a laminate
E = Young's modulus
f = frequency (cycles/second)
h = beam thickness
I = second moment of area of beam
k_t = transverse thermal conductivity (in thickness direction)
L = beam length
m = end-mass, cosine of ply (fiber) orientation
n = sine of ply (fiber) orientation
T = absolute temperature
t = time
w = beam width
W = maximum elastic energy stored during a cycle
ΔW = mechanical energy dissipated per cycle
x = coordinate along the length of the beam
y = amplitude of transverse vibration
α = linear coefficient of thermal expansion, eigenvalue
β = eigenvalue
δ = logarithmic decrement
ϵ_ψ = accuracy of experimental damping measurement
$\zeta = \xi$ = damping ratio
η = loss factor
λ = eigenvalue
ρ = density per unit volume of beam material
τ = relaxation time
ϕ = phase angle by which the applied stress leads the resulting strain
ω = frequency (radians/second), $2\pi f$
ω_o = resonant frequency of beam without an end-mass
ψ = damping = $\Delta W/W$
()' = real part of a complex quantity ()
()" = imaginary part of a complex quantity ()

1.0 INTRODUCTION

The design of any structure requires the quantitative knowledge of many parameters pertaining to the material of which the structure is built. Two parameters of importance in the analysis of structures subject to dynamic loads are the dynamic modulus and damping capacity. The measure of these entities, particularly damping, depends on the type of dynamic loading applied. Intrinsic, or material damping, is defined herein as the dissipation of energy within a material through the excitation of internal defect phenomena by the application of a homogeneous strain

field. Structural damping on the other hand, is composed of both intrinsic (material) and extrinsic (structural) components, and is defined to be the dissipation of energy produced by the application of a non-homogeneous strain field which is determined by specimen shape and structural application. Hence, a specimen subject to uniaxial tensile or compressive loading deforms and dissipates energy under a homogeneous strain field and therefore yields a measurement of intrinsic material damping. However, the strain field in a beam of the same material subject to flexural oscillations varies in the thickness direction and with position along the beam; this variation depending on boundary conditions. Therefore, energy dissipation within the beam will also be a function of thickness and position along the length of the beam, and will give a measure of structural damping. An example of such damping is the transport of thermal currents across the thickness dimension of a beam (Zener or thermoelastic relaxation).

Many experimental techniques have been proposed and developed to measure the dynamic constitution of materials. The technique described herein determines the dynamic properties in flexure with speed, automation, and measures of accuracy and precision. The experimental apparatus consists of a beam specimen mounted under cantilevered boundary conditions and vibrated in first-mode flexural resonance. Data acquisition and reduction techniques entail accurate determination of the resonant frequency, and a measure of the rate of decay in free-vibrational amplitude using a logarithmic decrement method for ascertaining the dynamic flexural modulus and structural damping, respectively[1].

Results pertaining to the flexural modulus and structural damping of 6061 aluminum and a symmetric four-ply metal-matrix composite composed of pitch-55 graphite fibers in a 6061 aluminum matrix are presented. These results are compared with those predicted by Euler-Bernoulli, Zener (thermoelastic), and laminate theories and show good agreement. End-masses were used to vary the resonant frequency of the test specimens[2]. A brief overview of the end-massed beam analysis and experimental results is presented to show that the addition of an end-mass only alters the resonant frequency of the specimen and does not contribute to the measure of damping. Damping results are presented in the form $\psi = \Delta W/W$, where ΔW is the energy dissipated during each loading cycle and W is the maximum energy stored. Calibration of the cantilevered configuration for apparatus losses was carried out in two steps. First, the damping of fused quartz, a material possessing negligible damping, was measured in a free-free apparatus[1]. This yielded a determination of the free-free apparatus losses. Second, flexural damping data for annealed 6061 aluminum obtained from both free-free and cantilevered configurations were compared. Results showed that, within the range of experimental

scatter, both configurations provided the same measure of damping. This agreement of the data justified equating the cantilevered apparatus losses to those of the free-free configuration. Accuracy of the experimental dynamic flexural modulus values was dependent upon the measurement of the resonant frequency and specimen parameters. An estimate of accuracy was obtained by comparing the results of the present study with those of an experimental study using ultrasonic wave propagation[3]. A These procedures determined accuracy of the modulus and damping values to be 0.1 percent and ϵ_ψ=3.0x10^{-4}, respectively. It is noted that ϵ_ψ is a systematic error and ϵ_ψ>0. Statistical analysis of all experimental data ascertained the precision to be 0.1 percent and 5x10^{-4} (one standard deviation), for modulus and damping, respectively.

2.0 SPECIMENS

A variety of specimens were tested including annealed 6061 and 6061T6 aluminum alloys, magnesium-0.6% zirconium alloy, magnesium-1% manganese alloy, leaded and lead-free brass, fused quartz, and three metal-matrix composite laminates, one comprising continuous pitch-55 graphite fibers (P55Gr) in a matrix of 6061 aluminum (P55Gr/6061Al), the second P55Gr fibers in a matrix of magnesium with 0.6 percent zirconium (P55Gr/Mg-0.6%Zr), and the third was constructed of P55Gr fibers in a matrix of magnesium with one percent manganese (P55Gr/Mg-1%Mn). The P55Gr/6061Al specimens were cut from a four-ply, balanced, symmetric, laminated plate at angles ranging from zero to ninety degrees in fifteen degree increments; in a zero degree specimen, the fibers are aligned along the length dimension of the beam. The P55Gr/Mg-0.6%Zr and P55Gr/Mg-1%Mn specimens were cut from a zero-degree, eight-ply laminate.

The P55Gr/6061Al diffusion bonded laminated composite beam specimens were constructed of four orthotropic, unidirectional lamina oriented at specific angles to the longitudinal beam axis and symmetrically disposed to the midplane of the laminate. During the fabrication process Gr/Al precursor tows each containing 2000, 10 μm diameter fibers were consolidated between 0.089 mm thick 6061 aluminum face sheets at the angles appropriate to the particular laminate layup. The laminate was processed at 588°C and 24.1 MPa for 20 minutes, yielding a composite plate of 50% fibre volume. Two specimens of each laminate orientation were tested. Specimen dimensions for the 6061 aluminum and metal-matrix laminate specimens are given in Table 1.

3.0 EXPERIMENTAL APPARATUS

A schematic diagram of the experimental apparatus utilized in this research is presented in Figure 1. This equipment determines the dynamic properties in flexure with speed, automation and measures of accuracy and precision. The apparatus consists of a beam specimen supported under cantilevered boundary conditions and vibrated in first-mode flexural resonance, a Wavetek Model 164 frequency generator, a Bruel and Kjaer electromagnetic transducer, a power amplifier for increasing the signal received by the transducer, a Micro-Measurements BAM-1 strain bridge, a Data Precision Model 6000/611 waveform analyzer, and a Hewlett Packard 9000/217 computer connected to the Data 6000 by an IEEE 488 interface. To isolate the system from the effects of air damping, the specimen was mounted in a vacuum chamber connected to a Cenco Hypervac 25 vacuum pump capable of drawing a hard vacuum of 0.013 Pa.

4.0 THEORETICAL BACKGROUND

To preserve the succinct nature of the paper only the final results of the Euler-Bernoulli, logarithmic decrement, thermoelastic, and laminate theories entailed in these studies will be given here.

4.1 Dynamic Flexural Modulus

Let ω' be the frequency of a cantilevered beam made of an isotropic anelastic material, and E' be the real part of the Young's modulus. By the use of the Correspondence Principle of linear viscoelasticity[4], and the Euler-Bernoulli theory of flexure, the relationship between E' and ω' is given by:

$$\omega' = \frac{\alpha^2}{L^2}\sqrt{\frac{E'I}{\rho A}} \qquad (1)$$

where $()'$ denotes the real part of a complex quantity, α is the eigenvalue, which for the fundamental mode of a cantilevered beam has a value of 1.875, E is the Young's modulus, I is the second moment of area, ρ is the density per unit volume, and A is the cross-sectional area. This analysis assumes that the free vibrations of low-loss viscoelastic materials are approximately harmonic[5].

4.2 Logarithmic Decrement

The logarithmic decrement technique entails measuring the rate at which the free-vibration amplitude decays with time. An

expression for the damping is given by:

$$\psi = \frac{\Delta W}{W} = \frac{4\pi \ln[A(t_1)/A(t_2)]}{\omega_r[t_2 - t_1]} \qquad (2)$$

where ω_r is the resonant frequency, and $A(t_1)$ and $A(t_2)$ are the peak displacements at times t_1 and t_2, respectively. In accordance with equation (2), $\ln[A(t_1)/A(t_2)]$ was plotted against (t_2-t_1), the least squares method was used to fit a straight line, and from the slope, m, of the straight line, the damping was calculated from:

$$\psi = 4\pi m/\omega_r \qquad (3)$$

Several other definitions of damping currently appear in the literature. For the convenience of the reader, their interrelationship is documented here:

$$\psi = 2\pi\tan\phi = 2\pi\eta = 4\pi\zeta = 4\pi\xi = 2\pi Q^{-1} = 2\pi E''/E' = 4\pi\omega''/\omega' = 2\delta$$

4.3 Thermoelastic (Zener) Damping

The variation of damping with frequency due to the transport of thermal currents as determined from Zener theory[6] is given by:

$$\psi = \psi_o \left[\frac{\omega\tau}{1 + \omega^2\tau^2}\right] \qquad (4)$$

where $\psi_o = \frac{2\pi\alpha^2 ET}{\rho C_p}$ and $\tau = \frac{h^2 \rho C_p}{\pi^2 k_t}$

Equation (4) describes the damping in a beam produced from the transport of thermal currents across the thickness dimension. This form of energy dissipation is dependent on the structural configuration and is produced by a non-homogeneous strain field. It is therefore a form of structural damping. This equation has been used in calculating the curves in Figures 4, 6 and 7.

4.4 Laminate Theory

The following expressions for flexural modulus and damping for a balanced, symmetric, laminated composite beam were derived using general plate theory of laminated composites[7] and the studies of Ni and Adams[8], respectively. It is noted that this laminate theory is based on the theory of linear elasticity and does not include thermoelastic effects. The coordinate system of the lamina (on-axis, principal, [1,2,3]) and laminate (off-axis, [x,y,z]), and the laminate ply counting sequence are shown in

Figures 2 and 3, respectively. The effective flexural modulus in free-flexure, where bending-twisting coupling is not constrained, is given by:

$$E_f = \frac{12}{h^3 D'_{11}} \tag{5}$$

Although it is obvious that the boundary conditions used do not constrain bending-twisting coupling (except at the clamped-end), this constraint was investigated for confirmation and completeness. The constrained flexural modulus, termed pure-flexure, is given by:

$$E_p = \frac{12D'_{66}}{h^3[D'_{11}D'_{66} - (D'_{16})^2]} \tag{6}$$

where D_{ij}' are components of the laminate flexural modulus matrix.

The total flexural damping is given by:

$$\psi = \psi_1 + \psi_2 + \psi_{12} \tag{7}$$

where $\psi_1 = \frac{\Delta W_1}{W}$ $\psi_2 = \frac{\Delta W_2}{W}$ $\psi_{12} = \frac{\Delta W_{12}}{W}$

$$\psi_1 = \frac{\psi_L}{3D'_{11}} \sum_{k=1}^{n} m^2(\bar{Q}_{11}D'_{11} + \bar{Q}_{12}D'_{12} + \bar{Q}_{16}D'_{16}) \\ (m^2D'_{11} + mnD'_{16})(h_k^3 - h_{k-1}^3)$$

$$\psi_2 = \frac{\psi_T}{3D'_{11}} \sum_{k=1}^{n} n^2(\bar{Q}_{11}D'_{11} + \bar{Q}_{12}D'_{12} + \bar{Q}_{16}D'_{16}) \\ (n^2D'_{11} - mnD'_{16})(h_k^3 - h_{k-1}^3)$$

$$\psi_{12} = \frac{\psi_{LT}}{3D'_{11}} \sum_{k=1}^{n} mn(\bar{Q}_{11}D'_{11} + \bar{Q}_{12}D'_{12} + \bar{Q}_{16}D'_{16}) \\ (2mnD'_{11} - [m^2-n^2]D'_{16})(h_k^3 - h_{k-1}^3)$$

and $m=\cos\theta_k$ and $n=\sin\theta_k$. The above relations were derived assuming negligible shear deformation and rotary inertia (Euler-Bernoulli beam theory) which holds for length-to-thickness ratios greater than approximately 30^9. The length-to-thickness ratio for the composite specimens tested was of the order of 100.

5.0 EXPERIMENTAL PROCEDURE

Vibrational motion of the beam specimen was induced using an electromagnetic transducer driven at the resonant frequency of the specimen. As the specimens were non-magnetic, a small, high permeability disc was attached to the end of the specimens to provide coupling with the transducer. The cyclic signal representing the motion of the specimen was obtained via a strain gage attached near the root. This gage was connected to the direct-current strain bridge, whose analog voltage output was passed to the Data 6000 acquisition device. When the specimen reached steady-state, forced vibrational motion, the resonant frequency was recorded by the computer. The current to the excitation transducer was then interrupted and the specimen went into free vibrational decay. The steady-state and the free-decay motion were recorded in digital form by the Data 6000 where the voltage of each positive peak of the waveform was determined and passed via the IEEE 488 bus to the computer.

In order to study the variation of dynamic flexural modulus and structural damping with frequency, an end-mass was attached to the end of the specimen to facilitate the variation of its resonant frequency[2]. The dynamic flexural modulus was calculated using equation (1) and the experimental values of resonant frequency and specimen parameters. Structural damping was determined using equations (2) and (3).

6.0 EXPERIMENTAL ERROR

Calibration of the cantilevered configuration for apparatus losses was carried out in two steps. First, the damping of fused quartz, a material possessing negligible damping, was measured in a free-free apparatus[1]. A reported damping value for fused quartz is 1.2×10^{-6} [10]. The value measured using the free-free vibrational apparatus was 3×10^{-4}. As the cited value is negligibly small, 3×10^{-4} is determined to represent apparatus losses, and is denoted ϵ_ψ. Therefore, the measured value of damping of any material using this apparatus can be decomposed into the thermoelastic (Zener) and intrinsic damping of the material plus apparatus losses:

$$\psi^{\text{free-free}}_{\text{measured}} = \psi^{\text{free-free}}_{\text{Zener}} + \psi_{\text{intrinsic}} + \epsilon^{\text{free-free}}_{\psi} \qquad (8)$$

Because it is impractical to measure the damping of fused quartz using a cantilevered apparatus due to the required clamping pressures and the fragile nature of the material, a comparison between measured damping values for annealed 6061 aluminum in

both free-free and cantilevered configurations was carried out. As shown in Figure 4, results displayed a negligible difference in the mean damping values obtained from the two techniques. The standard error for the least squares curve fit of all the data was 5×10^{-4}. In an analogous manner to that used for the free-free apparatus, the measured damping value of a material can again be decomposed according to equation (8):

$$\psi_{measured}^{cantilever} = \psi_{Zener}^{cantilever} + \psi_{intrinsic} + \epsilon_{\psi}^{cantilever} \qquad (9)$$

As the intrinsic damping of a material is a constitutional property, and the thermoelasic (Zener) damping is the same for both configurations, as comparison was made at the same frequency using specimens of the same dimensions, therefore:

$$\psi_{Zener}^{free\text{-}free} = \psi_{Zener}^{cantilever} \qquad (10)$$

Since the measured values of damping obtained from two different techniques agree over the range of frequencies and strain amplitudes studied, it follows from equations (8), (9) and (10) that

$$\epsilon_{\psi}^{free\text{-}free} = \epsilon_{\psi}^{cantilever} \qquad (11)$$

Therefore, from equation (11) and the agreement between the experimental results shown in Figure 4, the apparatus losses of the cantilevered configuration can be equated to the measured value of extraneous losses in the free-free apparatus; that is, for both configurations, the accuracy in the measurement of damping, defined by ϵ_{ψ}, is 3.0×10^{-4}. An additional point of interest obtained from Figure 4 is that the value of Zener damping, which is strain amplitude independent, lies within the range of intercept of the least squares best-fit straight line and the lines specifying the standard error. This adds credence to the measured data, and also demonstrates that, for the particular material tested where intrinsic damping is very low, an accurate measure of the intrinsic damping cannot be determined from the flexural damping as it lies within the range of experimental scatter. However, one may put bounds on its magnitude; that is $0 < \psi_{intrinsic} < 5 \times 10^{-4}$.

Accuracy of the experimental dynamic flexural modulus values is dependent upon the measurement of the resonant frequency and specimen parameters. A measure of the accuracy and precision of the modulus data was determined by calculating the modulus from thirty independent tests in which the resonant frequency was disturbed by attaching different end-masses to the end of a speci-

men[2]; this will be discussed further in the next section. Evaluation of the dynamic flexural modulus from the thirty different experimental values of frequency, and the corresponding eigenvalues determined from the end-mass used, resulted in a mean value of 69.376 GPa ± 0.1% (one standard deviation). This agrees within 0.1% with the value of 69.439 GPa ± 0.1% obtained from an independent study using ultrasonic wave propagation[3].

Thus, the accuracy of the measured modulus and damping values presented herein are 0.1 percent and 3.0×10^{-4}, respectively. Precision of the experimental data was ascertained to be 0.1 percent and 5×10^{-4} (one standard deviation), for modulus and damping, respectively.

7.0 RESULTS AND DISCUSSION

For continuity the essential results pertaining to the attachment of an end-mass to a beam specimen to facilitate the variation of resonant frequency are reproduced from[2]. This technique was used to determine the frequency dependence of dynamic flexural modulus and structural damping for the specimens tested. The data, covering almost two decades of frequency, were obtained using five different beam lengths and six different end-masses. The length, mass and frequency matrix is shown in Table 2.

The relationship between the frequency and end-mass is given by equation (1)[2] where now the eigenvalues, α, are the solutions of the transcendental equation:

$$\frac{1 + \cos\alpha\cosh\alpha}{\alpha(\sin\alpha\cosh\alpha - \cos\alpha\sinh\alpha)} = \frac{m}{\rho AL} \qquad (12)$$

Figure 5 shows the normalized frequency as a function of normalized mass for annealed 6061 aluminum and justifies the applicability of Euler-Bernoulli beam theory in the analysis. Further, each experimental data point is an independent measure of the dynamic flexural modulus since the eigenvalues are specified by equation (12) and vibrational frequencies are experimentally determined. Thus, the modulus can be calculated via a rearrangement of equation (1). It is emphasized that each data point provides an independent determination of the modulus as all parameters in equation (1), except the eigenvalues, are experimentally measured. Evaluation of the dynamic flexural modulus from the thirty experimental data points resulted in a mean value of 69.376 GPa ± 0.1% (one standard deviation). This agrees very well with the value of 69.439 GPa ± 0.1% obtained from an independent study[3].

Figure 6 shows the normalized damping as a function of normalized frequency for 6061 aluminum. The vertical arrow points to the frequency common to five of the reference beam length/end-mass combinations (11.19 Hz). These five measurements lie in the range $\psi=0.81\times10^{-2} \pm 0.02\times10^{-2}$ ($\pm2.5\%$). It is important to note that this observation of precision agrees well with the value of 5×10^{-4} obtained from the independent study of comparative damping values for the free-free and cantilevered configurations. The experimental program was designed to cover a broad range of frequency values on either side of the Zener relaxation frequency $\omega\tau=1$ and, as shown, experimental results follow the Zener curve very well. Figure 7 displays the normalized damping as a function of normalized mass for four nominal frequencies, namely, 8, 11.19, 16, and 20 Hz. Clearly, within the bounds of experimental error, the damping is insensitive to the end-mass.

The dependence of flexural modulus and damping with ply-angle for the P55Gr/6061Al metal-matrix composite laminate specimens was investigated at fixed values of frequency (35 Hz) and strain amplitude ($55\mu\epsilon$). Two specimens of each ply-angle were tested. The experimental flexural modulus results and the curves defined by equations (5) and (6) are shown in Figure 8. Locations where only one symbol is shown indicate that agreement of the experimental data was within the size of the graphing symbol. The variation of the unconstrained (free) dynamic flexural modulus with ply-angle, as defined by equation (5), is illustrated as the solid line in Figure 8. This semi-empiricle curve was generated using experimental values of the longitudinal and transverse moduli, Poisson's ratio, and the resultant element value of the laminate flexural modulus matrix, D'_{11}, calculated from a laminate code. As the shear modulus was unavailable, this parameter was varied in the laminate code to give the least-squares best-fit curve through the experimental flexural modulus data. From this routine a longitudinal shear modulus value of 16.5 GPa was obtained. The curve for the constrained (pure) flexural modulus, as defined by equation (6), is shown as the dashed line in Figure 8. Comparison of the two curves indicate that flexure is best modelled by considering twisting due to the bending-twisting coupling terms to be unconstrained, as expected.

Prediction of laminate structural damping, as given by equation (7), was calculated from the laminate code using the experimentally determined value for G_{LT} (from the flexural modulus curve-fit), measured values of ψ_L, ψ_T, obtained from flexural damping experiments on zero and 90 degree specimens, and curve-fitting for ψ_{LT}. The theoretical curve and experimental data are shown in Figure 9. The curve shown was generated using an analogous least-squares best-fit routine as that used to determine G_{LT}. This resulted in a value of $\psi_{LT}=0.039$. Experimental results

indicate that within experimental scatter, laminate theory predicts the flexural modulus and damping in graphite-aluminum metal-matrix laminates reasonably well. Tables 3, 4 and 5 provide a summary of the experimentally determined mechanical properties of annealed 6061 aluminum, continuous Pitch 55 graphite fibers, and the P55Gr/6061Al metal-matrix composite specimens tested, respectively.

8.0 CONCLUSIONS

The cantilevered flexural resonance apparatus discussed herein facilitates the measurement of the dynamic flexural modulus and structural damping capacity of a material. The attachment of an end-mass does not contribute to measured values of flexural modulus or damping. Experimental values obtained for the flexural modulus and structural damping of annealed 6061 aluminum display good agreement with Euler-Bernoulli and Zener (thermoelastic) theories. Experimental results obtained from specimens cut from a four-ply, balanced, symmetric, P55Gr/6061Al metal-matrix composite laminate at angles ranging from zero to ninety degrees in increments of fifteen degrees indicated that the flexural modulus and structural damping varied with ply angle. The classical laminate theory of Ni and Adams[8] adequately predicts this variation. Accuracy of the modulus and damping values were determined to be 0.1 percent and ϵ_ψ=3.0x10^{-4}, respectively. Statistical analysis of all experimental data ascertained the precision to be 0.1 percent and 5x10^{-4} (one standard deviation), for modulus and damping, respectively.

ACKNOWLEDGMENT

The specimens and a small financial contribution of the research were provided by the Martin Marietta Aerospace Corporation, Denver, Colorado (Program Managers: Dr M.S. Misra and Dr S.P. Rawal).

9.0 REFERENCES

1. Wren, G.G., and Kinra, V.K., "An Experimental Technique for Determining a Measure of Structural Damping," Journal of Testing and Evaluation, Vol. 16, No. 1, January 1988, pp 77-85.
2. Wren, G.G., and Kinra, V.K., "On The Effect of End-Mass on Damping," to appear in Experimental Mechanics.
3. Kinra, V.K., Petraitis, M.S., and Datta, S.K., "Ultrasonic Wave Propagation in a Random Particulate Composite," Interna-

tional Journal of Solids and Structures, Vol. 16, pp 301-312, 1980.

4. Schapery, R.A., "Viscoelastic Behavior and Analysis of Composite Materials," Composite Materials, 2, edited by Sendeckjy, Academic Press, New York (1974).
5. Read, B.E., and Dean, G.D., The Determination of Dynamic Properties of Polymers and Composites, Adam Hilger, Bristol, England, 1978.
6. Zener, C.M., Elasticity and Anelasticity of Metals, University of Chicago Press, Chicago, 1948.
7. Halpin, J.C., Primer on Composite Materials, Technomic Publishing Co., Lancaster, 1984.
8. Ni, R.G., and Adams, R.D., "The Damping and Dynamic Moduli of Symmetric Laminated Composite Beams - Theoretical and Experimental Results," Journal of Composite Materials, Vol. 18, March 1984, pp 104-121.
9. Whitney, J.M., Structural Analysis of Laminated Anisotropic Plates, Technomic Publishing Co., Lancaster, 1987.
10. Kimball, A.L., and Schenectady, N.Y., "Vibration Prolems -Part V -Friction and Damping in Vibrations," Journal of Applied Mechanics, September 1941, pp A-135 to A-137.

TABLE 1 - SPECIMEN PARAMETERS

Specimen ID	L m x10²	w m x10²	h m x10²	ρ kg/m³ x10³	E_L GPa	Ψ ΔW/W x10²
0-1	13.10	1.214	0.211	2.41	156.10	0.35
0-2	13.08	1.212	0.208	2.41	160.65	0.4
15-1	13.18	1.089	0.208	2.43	124.38	1.03
15-2	13.23	1.146	0.203	2.41	125.48	0.9
30-1	13.03	0.955	0.208	2.43	74.39	2.0
30-2	13.20	1.143	0.211	2.41	72.81	1.8
45-1	15.21	1.217	0.208	2.41	47.09	2.35
45-2	15.24	1.212	0.208	2.38	45.78	2.1
60-1	13.13	0.957	0.211	2.41	36.13	2.6
60-2	13.51	0.955	0.211	2.41	35.51	2.7
75-1	15.47	1.212	0.203	2.43	37.37	2.25
75-2	13.59	1.214	0.203	2.43	36.82	2.35
90-1	13.18	1.146	0.203	2.43	36.68	1.6
90-2	13.30	1.140	0.203	2.43	36.47	1.5

TABLE 2 -THEORETICAL VALUES OF RESONANT FREQUENCIES FOR DIFFERENT LENGTH/END-MASS COMBINATIONS

beam length (cm)	end-mass (g) m_6 91.17	m_5 40.09	m_4 19.96	m_3 10.34	m_2 4.99	m_1 0.17
L_1 12.70	11.19	16.68	23.15	31.10	41.70	78.46
L_2 16.51	7.52	11.19	15.44	20.55	27.11	46.90
L_3 20.32	5.49	8.15	11.19	14.76	19.20	31.15
L_4 24.13	4.24	6.25	8.55	11.19	14.90	22.19
L_5 27.94	3.39	4.99	6.79	8.82	11.19	16.96

width=1.27 cm, thickness=0.162 cm

TABLE 3 - MECHANICAL PROPERTIES OF ANNEALED 6061 ALUMINUM

E GPa	G GPa	ν	ρ kg/m^3 x10^3	α μm/m°K	k J/m°Ks	C_p J/kg°K
68.9	25.9	0.33	2.70	23.0	180.2	895.8

TABLE 4 - MECHANICAL PROPERTIES OF CONTINUOUS PITCH 55 CONTINUOUS GRAPHITE FIBERS

E_L GPa	E_T GPa	G_{LT} GPa	ν_{LT}	ρ kg/m^3 x10^3	α μm/m°K	k J/m°Ks
379.2	3.4	17.2	0.41	1.99	-1.25	120.9

TABLE 5 - EXPERIMENTALLY DETERMINED MECHANICAL PROPERTIES OF P55Gr/6061Al METAL MATRIX COMPOSITE

E_L GPa	E_T GPa	G_{LT} GPa	ν_{LT}	ρ kg/m^3 x10^3	V_f	ψ_L	ψ_T	ψ_{LT}
157.9	36.7	16.5	0.33	2.43	0.5	0.004	0.0155	0.039

V_f: volume fraction
ψ: $\Delta W/W$
Note: G_{LT} and ψ_{LT} were deduced from experimental results of flexural modulus and damping, respectively.

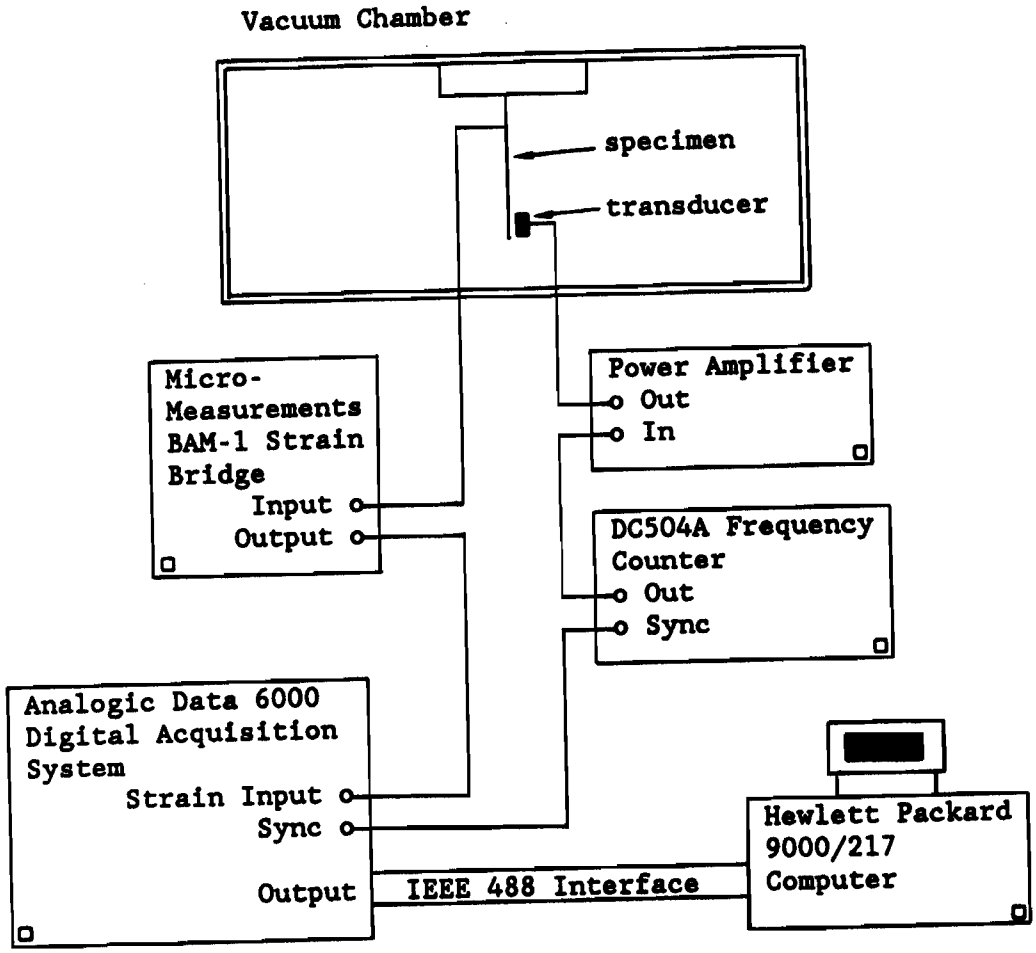

Figure 1 - Experimental Configuration

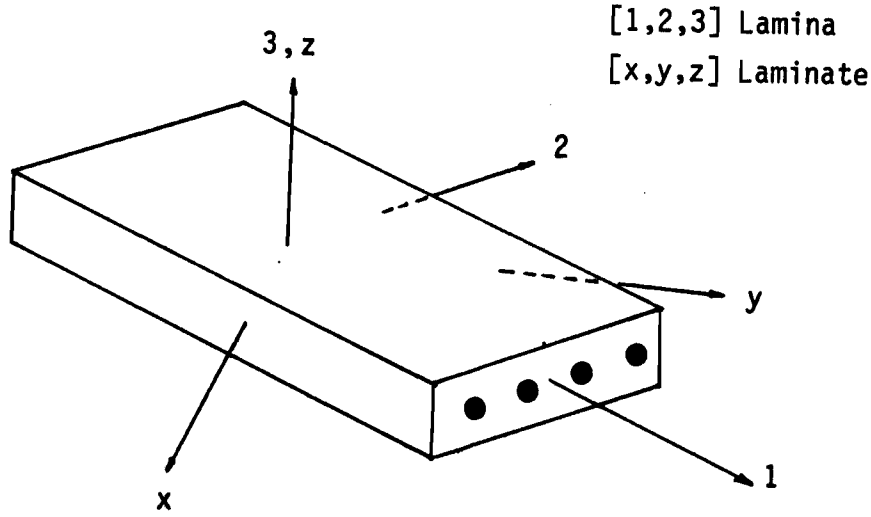

Figure 2 - Laminate Coordinate System

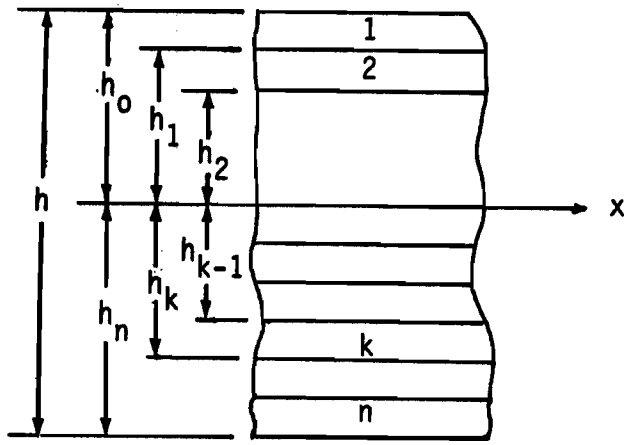

Figure 3 - Ply Counting Sequence

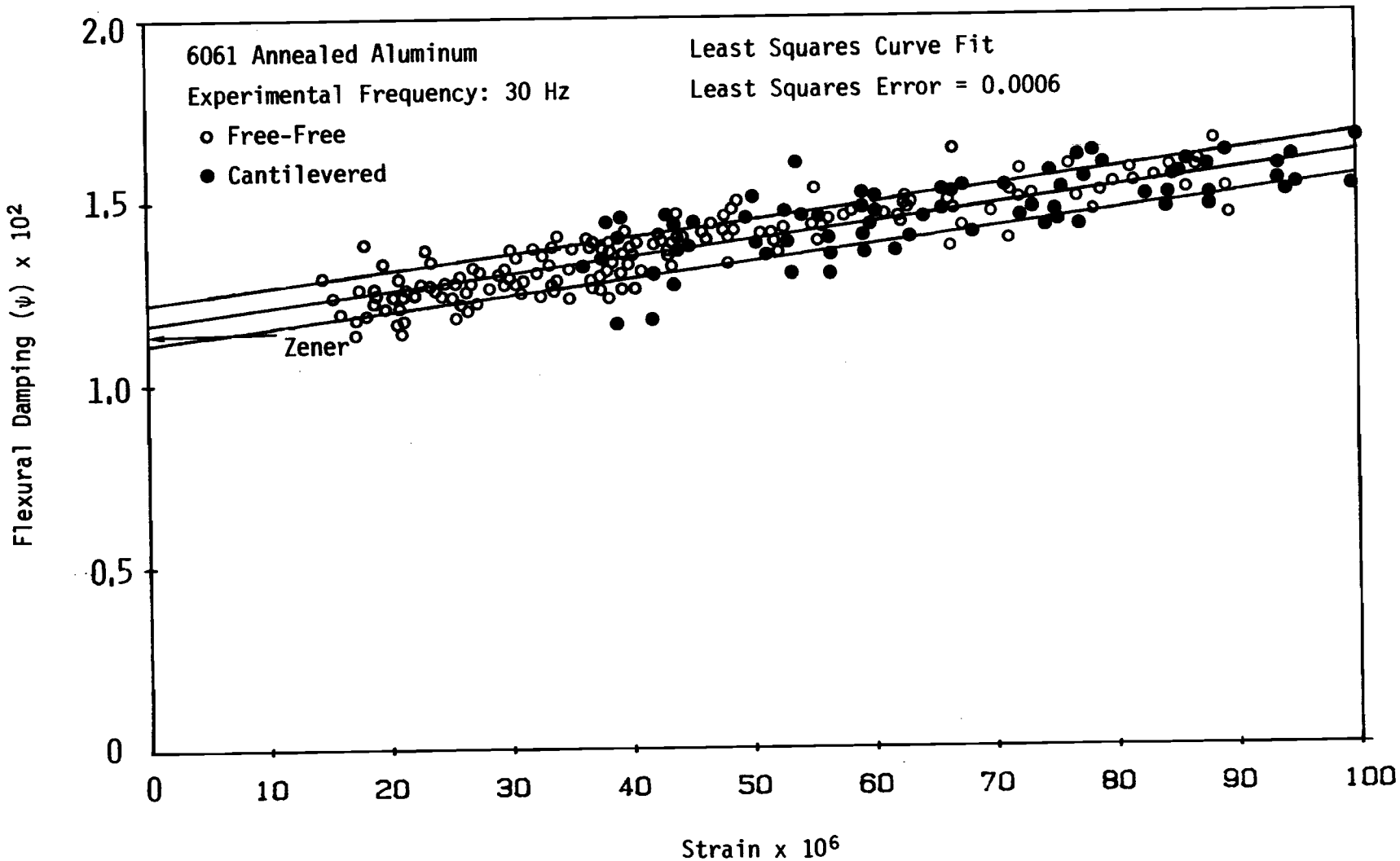

Figure 4 - Comparison of Flexural Damping Data from Free-Free and Cantilevered Configurations

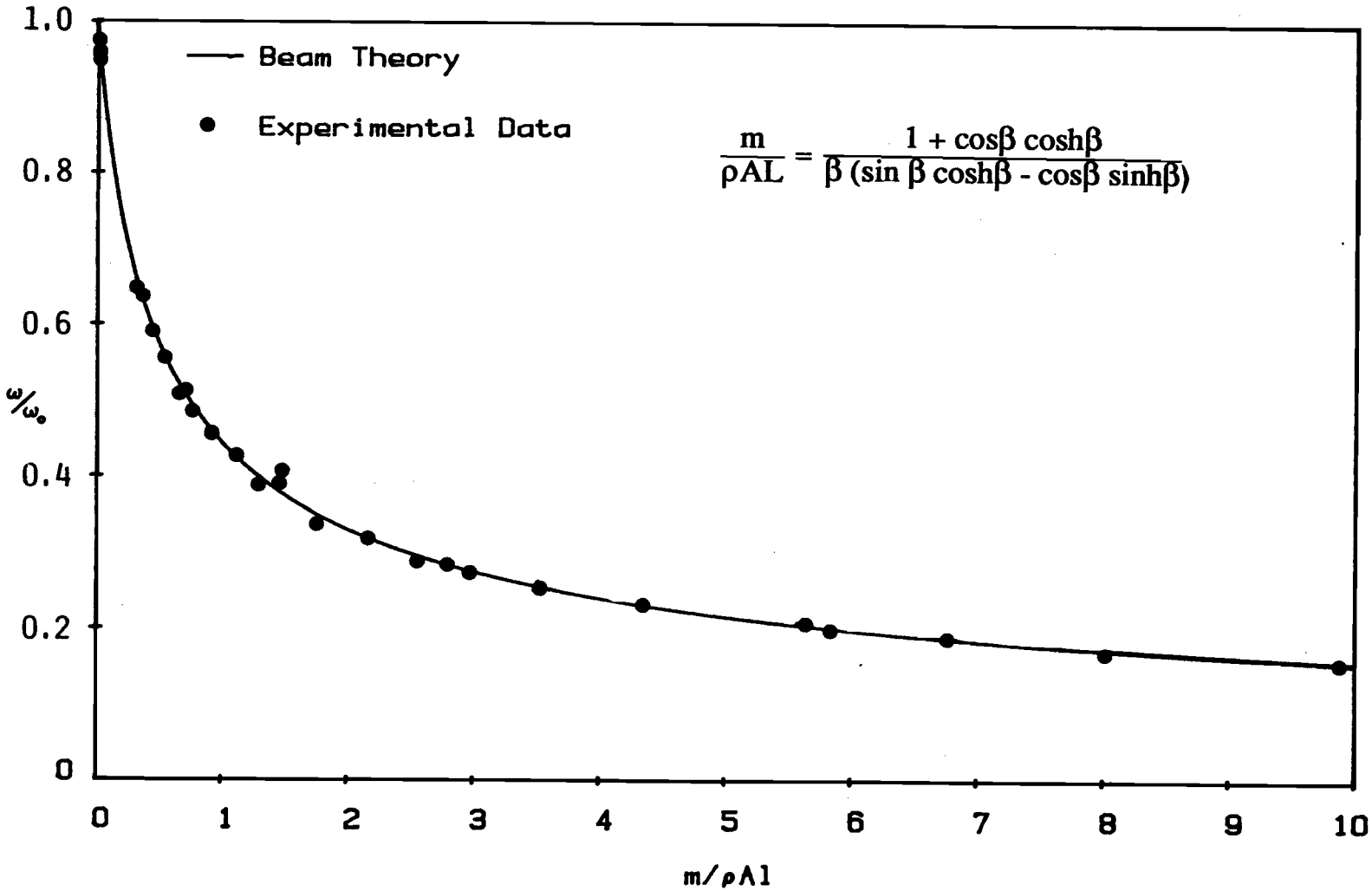

Figure 5 - The Effect of an End-mass on the Resonant Frequency of a Cantilevered Beam

HCA-20

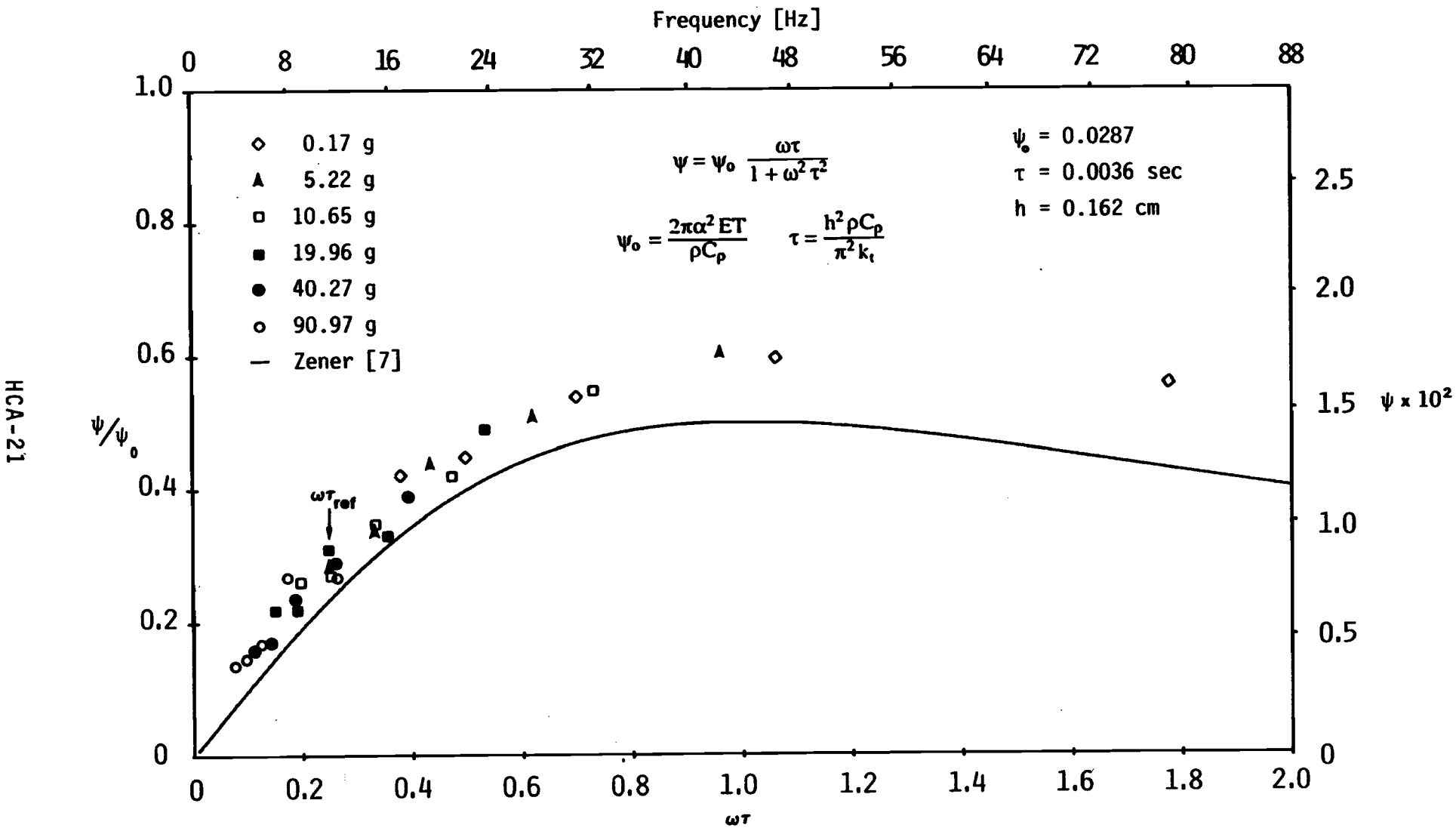

Figure 6 - Normalized Damping vs Normalized Frequency for 6061 Aluminum

Five beam lengths and six end-masses were chosen to produce the same resonant frequency (marked by arrow). Within the errors of measurement the measured damping does not depend on end-mass.

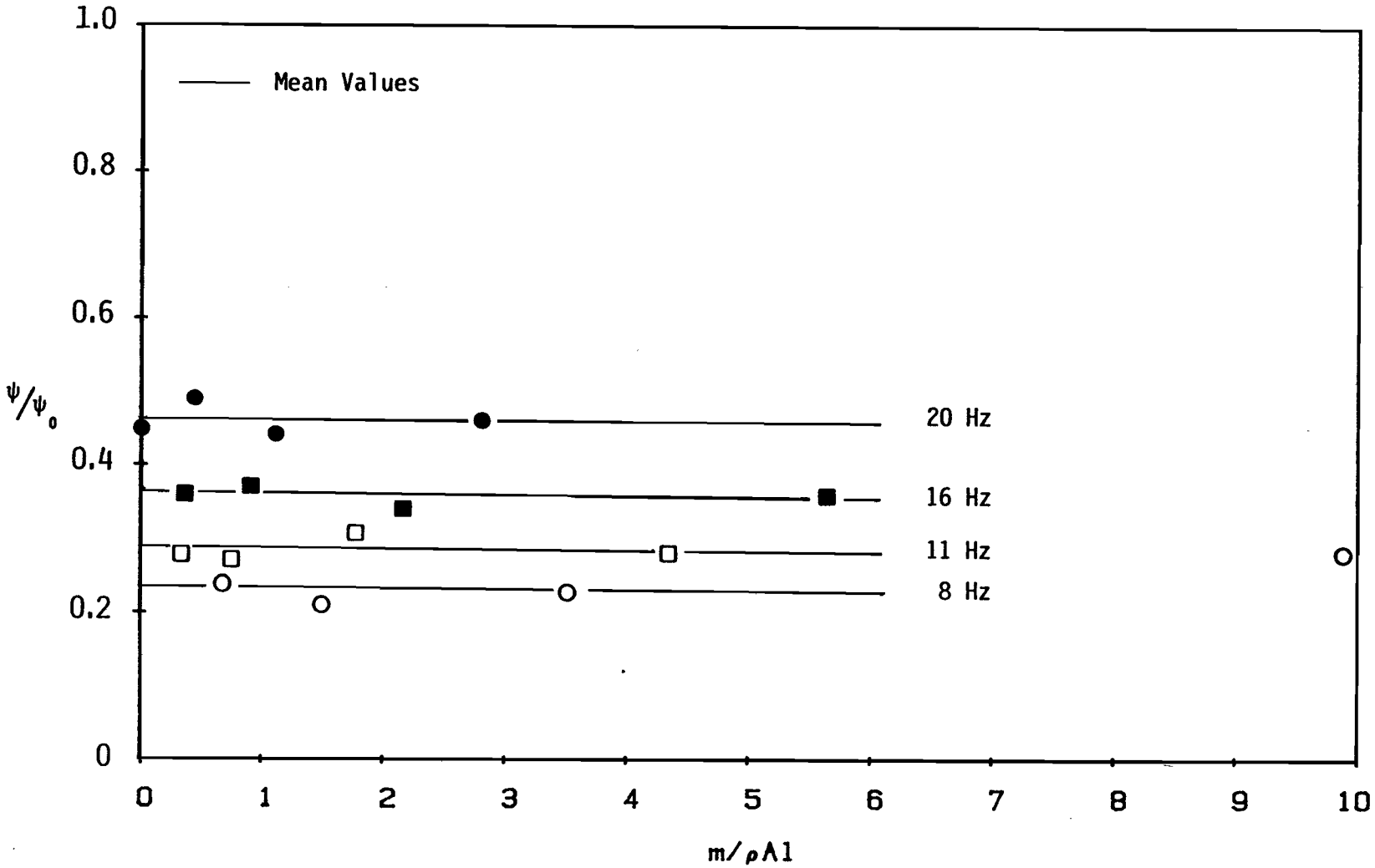

HCA-22

Figure 7 - Damping as a Function of End-mass for Four Nominal Frequencies

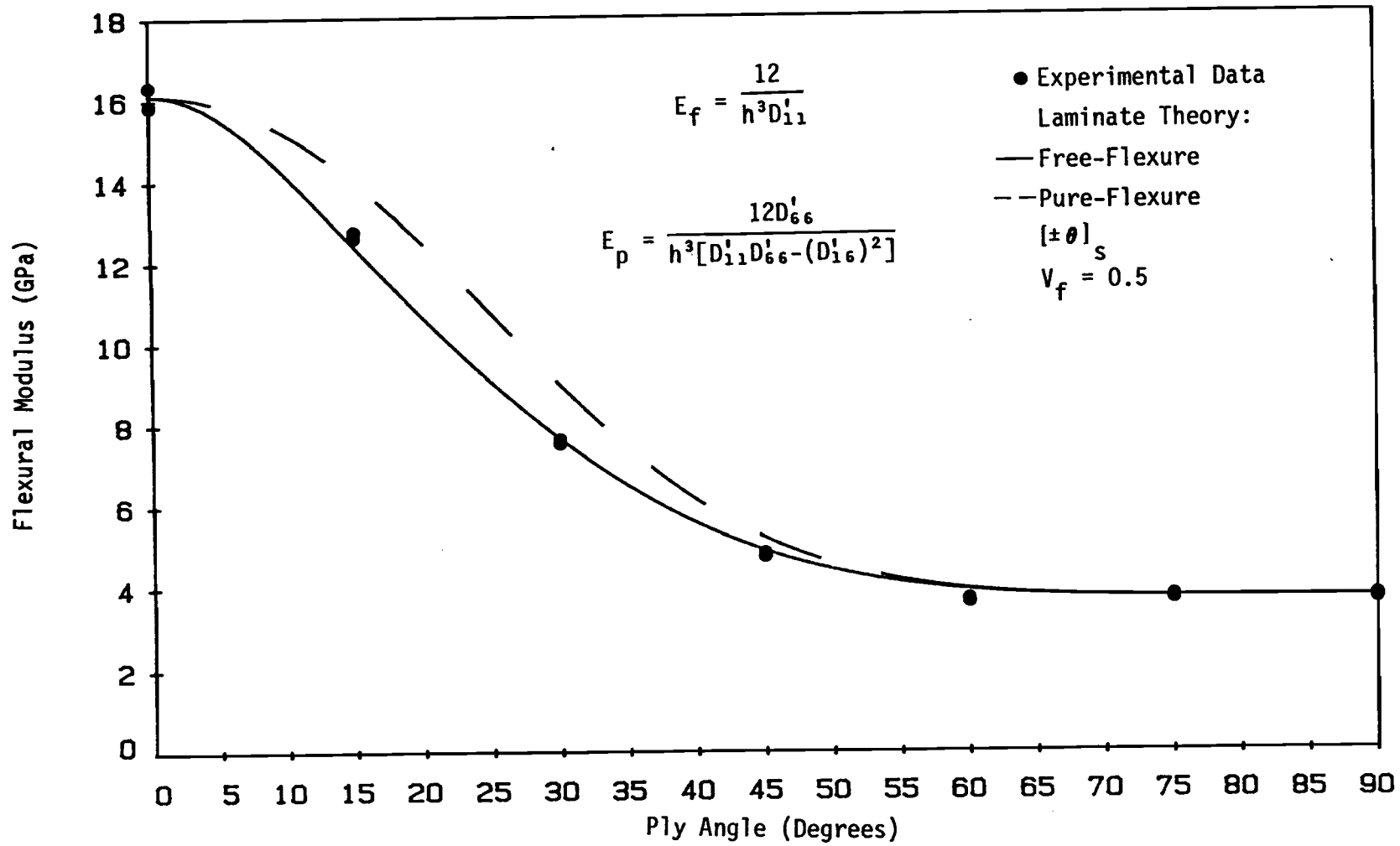

Figure 8 - Flexural Modulus vs Ply-Angle for Symmetric 4-Ply P55Gr/6061Al Composite

Two specimens of each ply angle were tested - the experimental data overlap

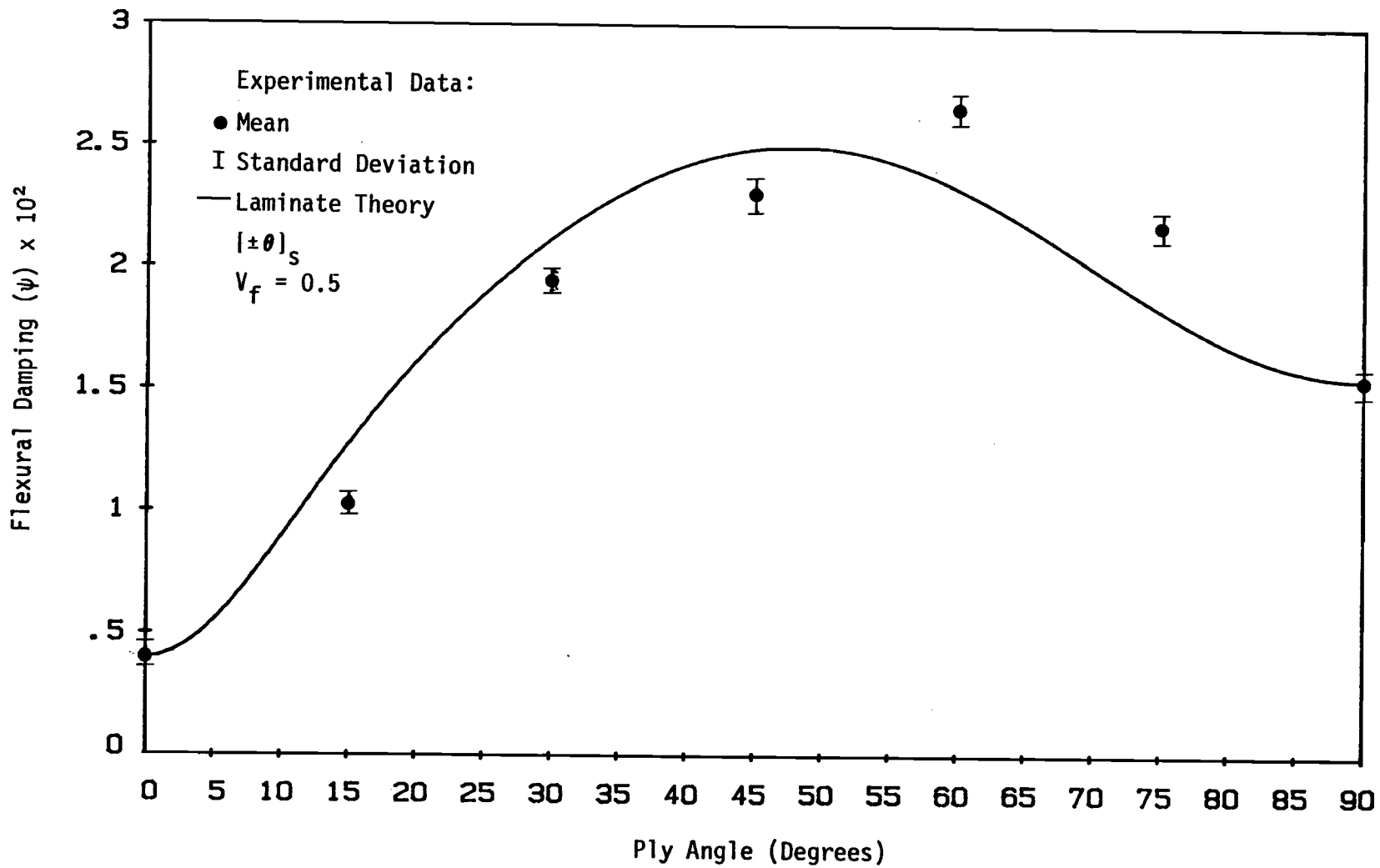

Figure 9 - Flexural Damping vs Ply Angle for Symmetric P55Gr/6061Al Composite